SYNAPSE 22:123–131 (1996)

In Vivo Studies of Acetylcholinesterase Activity Using a Labeled Substrate, *N*-[^{11}C]Methylpiperdin-4-yl Propionate ([^{11}C]PMP)

MICHAEL R. KILBOURN, SCOTT E. SNYDER, PHILLIP S. SHERMAN, AND DAVID E. KUHL
Division of Nuclear Medicine, Department of Internal Medicine, University of Michigan School of Medicine, Ann Arbor, Michigan 48109

KEY WORDS Mouse, Primate, Emission computed tomography, Carbon-11

ABSTRACT Two esters, *N*-[^{11}C]methylpiperidyl acetate ([^{11}C]AMP) and *N*-[^{11}C]methylpiperidyl propionate ([^{11}C]PMP), were synthesized in no-carrier-added forms and evaluated as in vivo substrates for brain acetylcholinesterase (AChE). After peripheral injection in mice, each ester showed rapid penetration into the brain and a regional retention of radioactivity (striatum > cortex, hippocampus > cerebellum) reflecting known levels of AChE activity in the brain. Regional brain distributions after [^{11}C]PMP administration showed better discrimination between regions of high, intermediate, and low AChE activities. Chromatographic analysis of blood and brain tissue extracts showed rapid and nearly complete hydrolysis of [^{11}C]PMP within 10 min after injection. For both [^{11}C]AMP and [^{11}C]PMP, retention of radioactivity in all regions was reduced by pretreatment with diisopropylfluorophosphate (DFP), a specific irreversible AChE inhibitor. DFP treatment also significantly increased the proportions of unhydrolyzed ester in both blood and brain. Radioactivity localization in brain after peripheral injection was thus dependent on AChE-catalyzed hydrolysis to the hydrophilic product *N*-[^{11}C]methylpiperidinol. PET imaging of [^{11}C]AMP or [^{11}C]PMP distributions in monkey brain showed clear accumulation of radioactivity in areas of highest AChE activity (striatum, cortex). These esters are thus in vivo substrates for brain AChE, with potential applications as in vivo imaging agents of enzyme action in the human brain. [^{11}C]PMP, the ester with a slower rate of hydrolysis, appears to be the better candidate radiotracer for further development.

INTRODUCTION

Alzheimer's disease (AD) has been proposed to result in selective loss of cholinergic neurons in the cortical regions of the human brain. This "cholinergic hypothesis" is supported by in vitro studies in post-mortem AD brains, where deficits of the enzymes choline acetyltransferase and acetylcholinesterase (E.C. 3.1.1.7) have been reported (Bierer et al., 1995, and references therein). A better understanding of the etiology and progression of AD, however, will require the development of methods to study the cholinergic system in living human brain, particularly early in the course of the disease. In recent years methods have been developed to image, using PET (positron emission tomography) and SPECT (single photon emission computed tomography), the distributions of specific radioligands for muscarinic cholinergic receptors (mAChR) (Dewey et al., 1990; Eckelman et al., 1984; Frey et al., 1991, 1992; Koeppe et al., 1994; Mueller-Gartner et al., 1992, 1993; Mulholland et al., 1992; Suhara et al., 1993; Varastet et al., 1992; Wilson et al., 1991), acetylcholine vesicular transporters (vAChT) (Kilbourn et al., 1990; Kuhl et al., 1994; Rogers et al., 1994; Widen et al., 1993) and the binding site of acetylcholinesterase (AChE) (Tavitian et al., 1993). Applications of such methods to AD have only recently begun to appear (Wyper et al., 1993; Yoshida et al., 1995; Zubieta et al., 1994).

An alternative approach to the study of AChE would be in vivo measurement of enzymatic activity, rather than the number of binding sites for a radiolabeled inhibitor such as [^{11}C]physostigmine. Recently, radiolabeled *N*-methylpiperidyl esters have been proposed as potential in vivo substrates of AChE; in the brain, these

Received March 20, 1995; accepted in revised form June 23, 1995.

esters are cleaved to yield *N*-methylpiperidinol, a more hydrophilic compound which is retained in the tissues (Irie et al., 1994; Namba et al., 1994). Administration of *N*-[^{14}C]methylpiperidyl esters to rats resulted in regional brain distributions of radioactivity which correlated with known distributions of AChE; similarly, PET imaging of the brain distribution of *N*-[^{11}C]methyl-3-piperidyl acetate ([^{11}C]MP3A) in monkey brain also showed a regional distribution consistent with AChE enzymatic activity. In rats, the accumulation of radioactivity in the frontal and parietal cortices after [^{14}C]MP3A administration was diminished (12–17%) by a lesion of the nucleus basalis magnocellularis (NBM), providing further support for an AChE-mediated localization mechanism (Namba et al., 1994).

We have recently synthesized a short series of *N*-[^{11}C]methyl-4-piperidyl esters (acetate, propionate, and benzoate esters) as potential in vivo imaging agents for AChE activity in the brain (Bormans et al., submitted for publication). Measurements of AChE activity would complement our current efforts at characterization of mAChR (Frey et al., 1992; Koeppe et al., 1994; Zubieta et al., 1994) and vAChT (Kuhl et al., 1994) in normal and diseased human brain; together, these radiotracer methods might provide a more complete description of the changes of the cholinergic system in AD brain. We report here that [^{11}C]PMP can be used as a metabolic trapping agent for the detection of AChE activity in the brain, and the regional rates of [^{11}C]PMP hydrolysis correlate well with both in vitro and in vivo measures of the cholinergic system. [^{11}C]PMP, in conjunction with external imaging with PET, will thus allow estimates of AChE activity in living primate and human brain.

MATERIALS AND METHODS

Radiotracer preparation

N-[^{11}C]methylpiperidyl acetate ([^{11}C]AMP) and *N*-[^{11}C]methylpiperidyl propionate ([^{11}C]PMP) were synthesized by *N*-[^{11}C]methylation of the 4-piperidinyl acetate and 4-piperidinyl propionate, respectively (Bormans et al., submitted for publication). Products were purified by HPLC and obtained in high specific activity (>500 Ci/mmol).

Regional in vivo mouse brain distributions: General procedure

Female CD-1 mice (20–25 g, Charles River) were anaesthetized with diethyl ester, and injected via the tail vein with a saline solution of radiotracer (100–400 μCi of [^{11}C]AMP or [^{11}C]PMP). Animals were allowed to awaken. After designated periods, animals were anaesthetized (ether) and decapitated, and the brain rapidly removed and immediately dissected into striatum (right and left striata combined), cortex (whole), hippocampus, hypothalamic region, thalamus, and cerebellum (Glowinski and Iversen, 1966). Tissue samples were counted for carbon-11 (automatic γ-counter) and weighed. Data were calculated as % injected dose/g tissue (%ID/g) and % injected dose/brain.

Brain distribution after diisopropylfluorophosphate (DFP) pretreatments

Mice (female CD-1, 20–25 g) were injected with 3 mg/kg i.p. DFP (Sigma Chemical Company, St. Louis, MO) freshly prepared as a solution in saline (Smolen et al., 1985, 1987). Three hours later, the regional brain distributions of [^{11}C]AMP and [^{11}C]PMP were determined using the procedure described above.

In vivo metabolism studies: General method

Female CD-1 mice (20–25 g; N = 2 per data point) were injected with 1–2 mCi of [^{11}C]PMP. Animals were sacrificed at 10 min, and samples of blood and whole brain rapidly removed and added to tubes containing 1 mL of absolute ethanol. Samples were homogenized and centrifuged. Supernatants were spotted on glass-backed silica gel plates (EM Science, Cherry Hill, NJ) and developed with 10% methanol in dichloromethane, with an ammonia atmosphere. Unlabeled standard PMP (R_f = 0.73) and N-methylpiperidinol (R_f = 0.29) were visualized with iodine. Radioactivity distribution on the plates was quantified using a Berthold Automatic TLC Linear Analyzer.

As a control experiment, [^{11}C]PMP was added to blood samples obtained from separate animals, and the blood subjected to the same chromatographic analysis as described above.

Primate imaging with PET

Single imaging studies of [^{11}C]AMP and [^{11}C]PMP were done in a female pigtail monkey (*M. nemistrina*, 4.6 kg). The animal was anaesthetized (15 mg/kg i.m. ketamine, repeated as necessary) and positioned in a TCC 4600A PET scanner (three-ring, five-slice tomograph); this PET scanner had been recently modified by addition of custom-fabricated lead collimators to provide improved spatial resolution (in-plane, 7.5 mm FWHM). Cerebral blood flow studies using i.v. injections of 3–5 mCi of ^{15}O-labeled water were done prior to the [^{11}C]ester studies, to aid in the positioning of the animal. Radiotracer ([^{11}C]AMP, 15.2 mCi; [^{11}C]PMP, 15.8 mCi) was injected via the femoral vein, and sequentially imaged (30-s frames early, progressing to 10 min frames at late times) for a total of 60 min.

Statistical methods

Significance of differences between groups of animals ([^{11}C]AMP vs. [^{11}C]PMP, and control vs. DFP-treated) were assessed using an unpaired Student's t-test. A value of $P < 0.05$ was considered significant.

TABLE I. Time course of regional mouse brain radioactivity distributions after i.v. injections of [^{11}C]AMP (top) and [^{11}C]PMP (bottom)

Brain region	[^{11}C]AMP, % ID/g			
	2 min	10 min	30 min	
Striatum	9.39 ± 1.6	11.3 ± 2.9	7.80 ± 0.87	
Cortex	8.96 ± 1.96	10.3 ± 2.7*	7.55 ± 0.52*	
Hippocampus	8.48 ± 1.76	9.66 ± 2.6*	7.36 ± 0.57*	
Hypothalamus[1]	8.54 ± 2.19	9.23 ± 2.79*	6.18 ± 0.38*	
Cerebellum	7.38 ± 1.08	6.40 ± 2.0*	4.03 ± 0.28*	
Thalamus	9.40 ± 1.8	10.8 ± 3.6*	6.41 ± 0.28*	
Blood	3.41 ± 0.46	1.86 ± 0.21	1.16 ± 0.04	
STR/CTX	1.05 ± 0.05	1.09 ± 0.08*	1.03 ± 0.14*	
STR/CBL	1.26 ± 0.03	1.79 ± 0.14*	1.94 ± 0.16*	
%ID/brain	4.35 ± 0.65	4.61 ± 1.28	3.31 ± 0.06*	
	[^{11}C]PMP, % ID/g			
Brain region	2 min	10 min	20 min	30 min
Striatum	12.9 ± 0.86	12.8 ± 2.7	8.68 ± 1.49	7.61 ± 1.3
Cortex	10.9 ± 1.31	8.4 ± 1.17	5.44 ± 0.65	5.13 ± 0.66
Hippocampus	10.5 ± 1.33	7.58 ± 0.96	5.49 ± 0.7	5.05 ± 0.73
Hypothalamus	8.67 ± 1.48	7.4 ± 0.9	5.58 ± 0.85	4.7 ± 0.55
Cerebellum	7.01 ± 0.97	4.2 ± 0.61	3.16 ± 0.63	2.51 ± 0.26
Thalamus	9.53 ± 1.1	8.67 ± 1.7	5.7 ± 1.12	4.41 ± 0.72
Blood	3.28 ± 0.26	1.94 ± 0.20	1.94 ± 0.94	1.02 ± 0.14
STR/CTX	1.18 ± 0.15	1.51 ± 0.22	1.58 ± 0.13	1.47 ± 0.15
STR/CBL	1.87 ± 0.34	3.04 ± 0.42	2.78 ± 0.27	2.86 ± 0.23
% ID/g brain	9.88 ± 1.1	7.92 ± 1.24	5.33 ± 0.76	4.73 ± 0.65

Each data point represents mean ± SD for N = 4 animals.
[1]Hypothalamic region by gross dissection.
*$P < 0.05$ vs. [^{11}C]PMP.

RESULTS

Regional mouse brain pharmacokinetics

Both [^{11}C]AMP and [^{11}C]PMP show distinct patterns of accumulation of radioactivity in the mouse brain, with highest levels in the striatum (STR), cortex (CTX), and hippocampus, with lower amounts in the cerebellum (CBL). With the exception of the striatum, concentrations of radioactivity in other brain regions and in the brain as a whole were significantly higher after [^{11}C]AMP (Table I). For both radiotracers, ratios of radioactivity between tissue regions did not change between 10 and 20 min. The STR/CBL and STR/CTX ratios were, however, significantly smaller for [^{11}C]AMP as compared to [^{11}C]PMP.

DFP effects on regional brain distributions

Pretreatment of animals with DFP significantly altered the regional brain radioactivity distributions of both [^{11}C]AMP and [^{11}C]PMP (Table II). For both radiotracers, radioactivity in STR, CTX, HIP, and CBL, as well as total brain radioactivity, were reduced from 35–60% as compared to control animals. Except for the STR/CTX ratio for [^{11}C]AMP, all other tissue concentration ratios for the two radiotracers were also significantly reduced.

Metabolite analyses

The total amounts of radioactivity and proportions of authentic [^{11}C]PMP and hydrophilic metabolite, *N*-[^{11}C]methylpiperidinol, in mouse blood at various times after i.v. injection were determined by chromatography. Blood levels of total radioactivity decrease from 2 to 30 min (Table I); TLC analysis of this radioactivity showed that even as early as 2 min after injection the radioactivity in the blood was predominantly the hydrolysis product (Fig. 1). By 30 min, radioactivity in blood was nearly completed (>95%) metabolite. That radiotracer hydrolysis occurred in vivo, and not during the tissue homogenization and extraction steps, was shown by the control experiments, where only a minor amount (<5%) of added [^{11}C]PMP was hydrolyzed during these procedures. Chromatographic analyses of brain radioactivity extracts showed a similar pattern: at 10 min the brain contained mostly the labeled metabolite with a very small amount of unhydrolyzed ester (<5%), and at 30 min the ester was barely detectable (<1%).

The distribution of radioactivity between unchanged [^{11}C]PMP and hydrolysis product was significantly altered by pretreatment with DFP (Fig. 2). In both blood and brain, there were large amounts of unhydrolyzed ester present in the brain at 10 min. Total blood radioactivity levels were not different (1.76 ± 0.02 and 1.90 ± 0.11% ID/g in control and DFP-treated mice, respectively).

PET imaging of monkey brain pharmacokinetics

Both radiotracers freely penetrated the blood-brain-barrier, and at the later time periods (>15 min) there was clearly higher retention of radioactivity in striatum relative to cortex or cerebellum. In contrast to the previ-

TABLE II. Regional mouse brain distributions of radioactivity determined 10 min after i.v. injections of [^{11}C]AMP and [^{11}C]PMP

	[^{11}C]AMP (N = 9)	[^{11}C]AMP + DFP (N = 6)	[^{11}C]PMP (N = 9)	[^{11}C]PMP + DFP (N = 5)
% ID/g				
Striatum (STR)	10.4 ± 2.3	5.78 ± 0.6*	11.7 ± 2.3	4.95 ± 0.4*
Cortex (CTX)	9.43 ± 1.9	5.16 ± 0.6*	6.87 ± 1.4***	4.34 ± 0.6*
Hippocampus (HIP)	8.91 ± 1.9	4.89 ± 0.6*	6.57 ± 1.2***	4.34 ± 0.7*
Cerebellum (CBL)	5.79 ± 1.4	3.89 ± 0.5**	4.34 ± 0.7***	3.15 ± 0.5*
Tissue concentration ratios				
STR/CTX	1.09 ± 0.08	1.13 ± 0.11	1.71 ± 0.19***	1.14 ± 0.09*
CTX/CBL	1.64 ± 0.12	1.32 ± 0.07*	1.79 ± 0.15***	1.38 ± 0.06*
STR/CBL	1.81 ± 0.20	1.49 ± 0.17**	3.06 ± 0.31***	1.58 ± 0.17*
% Injected dose in whole brain	4.42 ± 0.88	2.58 ± 0.23*	3.43 ± 0.56***	2.06 ± 0.21*

Distributions were determined with and without pretreatment with 3 mg/kg i.p. DFP, 3 h prior. Data are presented as mean ± SD. *$P < 0.005$; **$P < 0.05$ as compared to controls; ***$P < 0.05$ as compared to control [^{11}C]AMP.

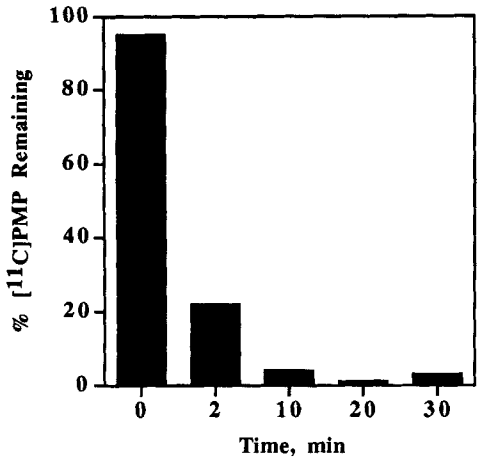

Fig. 1. Metabolite analysis of mouse blood at selected times after i.v. administration of [^{11}C]PMP. Bars represent remaining authentic [^{11}C]PMP, as determined by thin layer chromatography. The zero time point represents the in vitro radioactivity distribution in a sample of control blood spiked with [^{11}C]PMP. Each data point represents the average of two determinations.

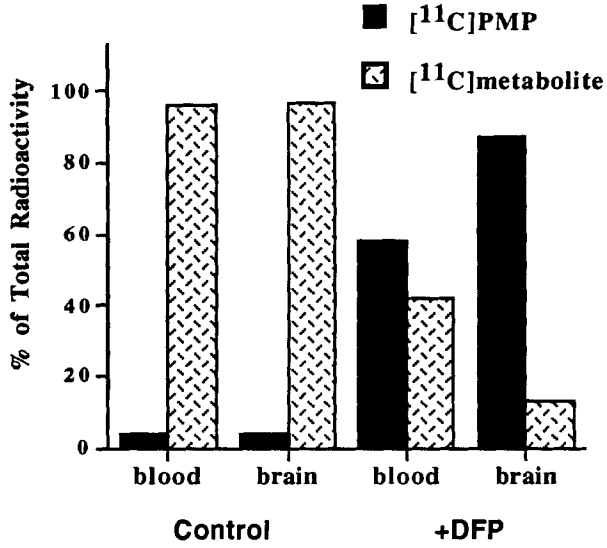

Fig. 2. Metabolite analysis of blood and brain following i.v. administration of [^{11}C]PMP to control and DFP-treated mice. Bars represent the average (N = 2) percentages of authentic [^{11}C]PMP and labeled metabolite, *N*-[^{11}C]methylpiperidinol, in tissues as determined by thin layer chromatography.

ous imaging of *N*-[^{11}C]methylpiperidin-3-yl acetate (Namba et al., 1994), we did not observe concentrations of activity in a region which could be assigned as the thalamus. For both [^{11}C]AMP and [^{11}C]PMP, regional brain levels of radioactivity and tissue concentrations ratios (STR/CTX) remained constant (corrected for decay) after approximately 15 min (Fig. 3). Throughout the imaging period, cerebellar radioactivity levels were lower than those seen in the cortex (data not shown). Significant differences were seen in both the shape of the tissue time-activity curves, as well as the relative amounts of radioactivity trapped in striatum and cortex. [^{11}C]PMP showed a high initial uptake in both striatum and cortex but a significant fraction of both striatal and cortical radioactivity (approx. 15% and 50%, respectively) washed out over the initial 15 min. In contrast, [^{11}C]AMP showed rapid tissue uptake but essentially no egress from the striatum, and a lower level (approx. 25%) of radiotracer loss from the cortex after the maximal uptake had occurred. Finally, as was seen in mice, there is a significantly better regional distinction between striatum and cortex for [^{11}C]PMP, with a maximal STR/CTX ratio of 2.25 after 15 min. This ratio never exceeded 1.8 after [^{11}C]AMP administration.

DISCUSSION

N-Methyl-4-piperidinyl esters are metabolic substrates for AChE, which upon hydrolysis form a metabolite (*N*-methylpiperidin-4-ol) that is essentially trapped within the brain tissues (Irie et al., 1994). Provided that not every radiotracer molecule delivered to the tissues is immediately and irreversibly hydrolyzed (which would make the radiotracer distribution delivery dependent, as discussed below), the tissue levels of metabolite should reach a level which reflects the relative proportion of active enzyme present. We believe one of our

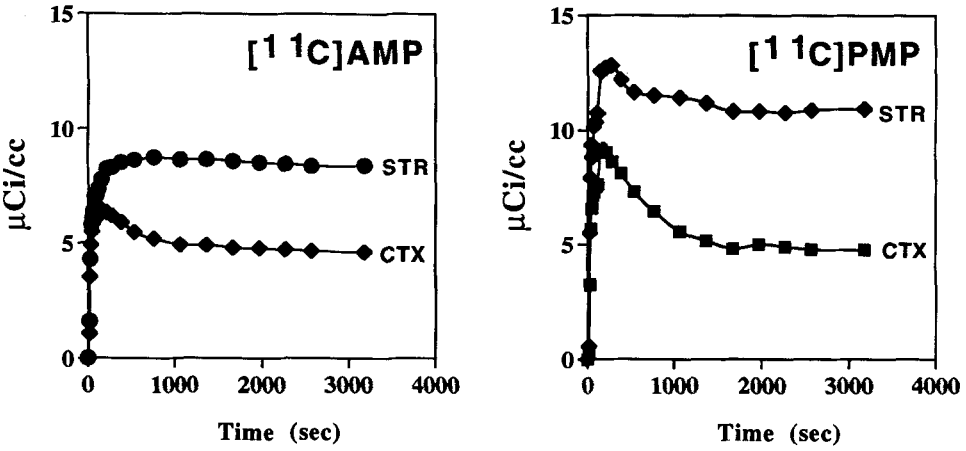

Fig. 3. Radioactivity time vs concentration curves for regions of interest placed over the striatum (STR) and cortex (CTX) of monkey brain. Radioactivity concentrations were determined by PET imaging following i.v. injections of [^{11}C]AMP (15.2 mCi) and [^{11}C]PMP (15.8 mCi).

new radiotracers, [^{11}C]PMP, fulfills these requirements for an in vivo tracer of regional AChE activity in the brain.

Among the possible piperidinol esters which might be labeled for in vivo use, we selected [^{11}C]AMP and [^{11}C]PMP as representing substrates with very high (AMP) and much lower (PMP) in vitro hydrolysis rates (Irie et al., 1994). In previous studies we had determined that the larger benzoate ester (chosen to provide an option for fluorine-18 labeling) is not cleaved at all by AChE in the brain. Labeling of PMP and AMP could be accomplished by simple *N*-[^{11}C]methylation of the piperidinyl esters, and as the products are non-chiral, there was no need for resolution of the two isomers which would result from synthesis of the corresponding 3-piperidinol analogs (such as *N*-[^{11}C]methylpiperidin-3-yl acetate; Namba et al., 1994); the stereochemical requirements for AChE hydrolysis of these esters has not been previously addressed, but AChE does show stereospecificity in the binding of competitive inhibitors (Chen et al., 1992).

The regional brain time-radioactivity distributions of [^{11}C]AMP and [^{11}C]PMP in mouse brain (Table I) were essentially identical to that previously reported using the carbon-14 labeled compounds (Irie et al., 1994). As previously reported, at later time points after peripheral injection the predominant radiolabeled species in mouse brain is the hydrolysis product (*N*-[^{11}C]methylpiperidinol), and thus the differences in radioactivity concentrations can be attributed to regional levels of AChE hydrolytic activity. The major differences between the two esters examined here were total brain retention of radioactivity at later times ([^{11}C]AMP > [^{11}C]PMP), and the uptake and retention of radioactivity in the cortex, hippocampus, and cerebellum, which show higher absolute levels for [^{11}C]AMP ($P < 0.05$ vs. [^{11}C]PMP at 30 min); striatal radioactivity retention was essentially equivalent for both radiotracers. The lack of distinction between the striatum and cortex for [^{11}C]AMP (STR/CTX = 1.09 ± 0.08) would be consistent with the greater in vitro hydrolysis rate for the acetate ester, and also suggests that the [^{11}C]AMP distribution into one or both of these tissues might be delivery limited. [^{11}C]PMP, which demonstrates a higher STR/CTX (1.79 ± 0.15) as well as a higher STR/CBL ratio (3.06 ± 0.31), thus appears to be a better candidate as an in vivo radiotracer for imaging.

To verify that the distributions of radioactivity in the brain were indeed due to the actions of AChE, we determined the regional radioactivity distributions in mice pretreated with the potent *irreversible* AChE inhibitor, diisopropylfluorophosphate (DFP). Regional brain distributions were determined at 10 min, since tissue ratios in control animals did not change after that time point. For both [^{11}C]AMP and [^{11}C]PMP, the injection of DFP (3 mg/kg i.p.) 3 h prior to radiotracer administration significantly reduced whole brain concentrations of radioactivity by 40% (Table II). The residual radioactivity concentrations in the DFP-treated mice could represent one or both of the following: 1) presence of *N*-[^{11}C]methylpiperidinol due to continued ester hydrolysis by remaining AChE after incomplete enzyme inhibition in the brain, or 2) presence of unhydrolyzed ester ("non-specific distribution") as a result of AChE inhibition. The continued accumulation of *N*-[^{11}C]methylpiperidinol, due to incomplete blocking of the enzyme, would be consistent with the reported 45–55% reductions of AChE activity determined ex vivo in mouse brain following a single 3 mg/kg i.p. injection of DFP (Smolen et al., 1985, 1987). The chromatographic examination of radioactivity in DFP-treated mice (Fig. 2) showed that, for [^{11}C]PMP, the brain contains both unhydrolyzed ester (87%) as well as the labeled hydrolysis product (13%); this suggests only partial blocking

of the brain AChE activity by the DFP dose employed. In DFP-treated mice it is also clear that the unchanged radiotracer, [^{11}C]PMP, persists in the blood for longer periods after injection (Fig. 2) and thus the total amounts of substrate delivered to the brain are also likely to have been altered through DFP inhibition of peripheral esterases. Whether a higher dose of DFP would result in larger decreases in brain radiotracer accumulation could not be tested, as animals given 5–6 mg/kg i.p. DFP did not survive; in addition, administration of 6.33 mg/kg i.p. DFP was found by Smolen et al. (1985) to still not produce complete inhibition of AChE in regions of mouse brain. It may not, in fact, be possible to determine non-specific distribution of these esters using complete AChE inhibition due to the lethal effects of total blockade of this enzyme, a problem we have noted before in attempts to utilize systemic administrations of highly toxic blocking agents of the cholinergic system (Kilbourn et al., 1990).

In contrast to radiotracer studies with radioligands for receptors or transporters, where pharmacological blockade of high affinity binding sites through peripherally administered blocking agents is generally assumed not to significantly change the non-specific distribution of the radioligand, these studies with AChE substrates and a systemic AChE inhibitor are more complicated to interpret. The difference between control and DFP-treated mice may not represent simply an estimate of total AChE activity due to the presence of unhydrolyzed ester in the brain of drug-treated animals (see above), but rather indicates the radiotracer distribution differences between control and partially blocked states; from the perspective of potential future applications for in vivo studies of AChE losses in disease, this is exactly what these radiotracers must be able to discriminate. The highly reactive substrate [^{11}C]AMP continues to fail to show any differences between striatum and cortex in the DFP-treated mice, and only a modest (−18%) reduction in the STR/CBL ratio (Table II), even in the partially blocked state. In contrast, [^{11}C]PMP (with a slower hydrolysis rate by AChE) demonstrates significant reductions of both the STR/CTX (−34%) and STR/CBL (−49%) ratios in the DFP-treated mice. Although it was not possible to determine, on a regional basis, the proportions of ester and hydrolysis product (insufficient radioactivity for chromatographic analysis), these results suggest that radioactivity distributions after [^{11}C]AMP injections may still be delivery-limited even after significant reductions in the numbers of AChE enzymes, and that [^{11}C]PMP will be better suited for detecting differences in AChE activities in vivo. As there was no unhydrolyzed ester observed in brain tissues of control mice at later time points after injection, it is also conceivable that the notion of "non-specific" distribution as usually considered for receptor or transporter radioligands would be irrelevant for these AChE substrates when tissue distributions at such latter time points are used as the semiquantitative estimates of AChE activity. These studies also demonstrate that the quantitative analysis of brain AChE enzymatic activity, and determination of enzyme inhibition by competing drugs, will require pharmacokinetic modeling approaches which account for the changes in the peripheral metabolism of these esters.

Acetylcholinesterase is but one component of the cholinergic system, and although a strict 1:1 regional correspondence with other cholinergic indices (muscarinic cholinergic receptors, vesicular acetylcholine transporter, choline acetyltransferase) might not be expected, in general there are good correlations between the regional brain distributions of these enzymes and transporter in normal brain. For both [^{11}C]AMP and [^{11}C]PMP, regional brain distributions of radioactivity in mouse brain at 10 min correlate reasonably well (correlation coefficients of 0.7 to 0.85 for [^{11}C]AMP) or quite well (coefficients > 0.95 for [^{11}C]PMP) with literature values for AChE and ChAT enzymatic activities (Gordon and Finch, 1984; Smolen et al., 1985, 1987), in vivo and in vitro radioligand binding to vAChT (Jung et al., 1990; Kilbourn et al., 1990), in vivo and in vitro numbers of mAChR (Virgili) et al., 1991; Wilson et al., 1991) and concentrations of ACh (Durkin et al., 1977). However, these correlations are based on four to five tissue regions (usually striatum, cortex, cerebellum, hypothalamus and hippocampus) and they do not suffice to demonstrate the most important differences between [^{11}C]AMP and [^{11}C]PMP, as the correlations are largely dependent on the differences between the regions of highest (STR) and lowest (CBL) AChE activity and are not very sensitive to the values for intermediary tissues such as cortex and hippocampus. More informative to consider are the STR/CTX ratios: although the many published in vitro and in vivo studies of AChE, ChAT, vAChT, and mAChR report widely varying absolute measures for these cholinergic functions (depending on species or strains of animals, and assay methods), there are consistently higher amounts of these cholinergic indices in the striatum, with STR/CTX ratios ranging from 1.6 to 10 in rodent brain. Using this ratio as the discriminating measure, [^{11}C]PMP (STR/CTX = 1.79) is considerably better than [^{11}C]AMP, which shows very little difference between these two tissues (STR/CTX = 1.19). This is consistent with the proposed delivery dependence of [^{11}C]AMP distributions, such that very similar amounts of this radiotracer are delivered to the striatum and cortex (with similar blood flows) and essentially all such tracer is immediately hydrolyzed and trapped in both tissues.

Based on these encouraging results in mice, we proceeded to investigate the regional brain kinetics of both [^{11}C]AMP and [^{11}C]PMP in primate brain, using i.v. bolus injections of radiotracer and PET imaging of radioactivity distributions. A single imaging study was done for each radiotracer, but using the same monkey and the

same injected dose of carbon-11. The goal of these studies was threefold: 1) to demonstrate brain penetration of these radiotracers in monkeys, sufficient for PET imaging; 2) to verify that the tissue time-activity curves would, at some point following injection, become essentially flat due to complete hydrolysis of ester in both the blood and brain; and 3) determine if there were significant differences between the in vivo pharmacokinetics of [^{11}C]AMP and [^{11}C]PMP. Both radiotracers freely penetrated the blood-brain-barrier, and at the later time periods (>15 min) there was clearly higher retention of radioactivity in striatum relative to cortex or cerebellum, consistent with the expected distribution of AChE in primate brain (Mesulam et al., 1984). In contrast to the previous imaging of *N*-[^{11}C]methylpiperdin-3-yl acetate (Namba et al. 1994), we did not observe concentrations of activity in a region which could be assigned as the thalamus. For both [^{11}C]AMP and [^{11}C]PMP, regional brain levels of radioactivity and tissue concentration ratios (STR/CTX) remained constant (corrected for decay) after approximately 15 min (Fig. 2), consistent with tissue trapping of the hydrolysis product. The flat tissue time-activity curves furthermore suggest, but do not prove, that there is not continuous delivery of substrate to the brain via the bloodstream. With the rapid in vivo hydrolysis of these esters in the brain, and the very large amount of esterases present in peripheral tissues, it is quite likely that monkey blood concentrations of these esters are very low (if existing) at later times after injection, as was seen in mice. In comparing the two radiotracers, significant differences were seen in both the shape of the tissue time-activity curves, as well as the relative amounts of radioactivity trapped in striatum and cortex. Again, consistent with the slower in vitro hydrolysis rate, the pharmacokinetics of [^{11}C]PMP show a high initial uptake in both striatum and cortex but a significant fraction of both striatal and cortical radioactivity washed out over the initial 15 min. In contrast, [^{11}C]AMP, which has a very high in vitro hydrolysis rate by AChE, shows rapid tissue uptake but essentially no egress from the striatum, and a lower level of radiotracer loss from the cortex after the maximal uptake has occurred. As was seen in mice, there is a significantly better regional distinction between striatum and cortex for [^{11}C]PMP, with a maximal STR/CIX ratio of 2.25 after 15 min. Finally, there was significantly more radioactivity trapped in the monkey brain following [^{11}C]PMP injection; this would be consistent with the higher lipophilicity of PMP and thus a greater brain extraction, but without knowing the relative blood concentrations for the two radiotracers, this difference in brain uptake cannot be so simply explained. We have not as yet applied any quantitative pharmacokinetic models to the PET data obtained with [^{11}C]AMP or [^{11}C]PMP; however, if metabolite-corrected arterial blood samples can be obtained such data could be analyzed using a pharmacokinetic model which calculates the irreversible blood-to-brain transfer constant (influx constant, K_i), as has been previously done for the irreversible monoamine oxidase inhibitor L-[^{11}C]deprenyl (Arnett et al., 1987). Efforts in this area will be reported in the future.

Our results, combined with the previous in vitro and in vivo investigations of these esters as AChE substrates (Irie et al., 1994; Namba et al., 1994), suggest that the development of in vivo imaging strategies for quantification of AChE in the human brain may be feasible. Of the two potential radiotracers examined here, [^{11}C]PMP is clearly superior, and can be used to discriminate between regions of high, intermediate, and low AChE activity. Considerable work remains to verify that the in vivo distribution of radioactivity after [^{11}C]PMP administration is not affected by drugs for other components of the cholinergic system, and that the ester is not bound significantly to any other receptor, enzyme, or transporter in the brain. Any in vivo binding of the hydrolysis product (N-[^{11}C]methylpiperidin-4-ol) would be inconsequential to the proposed imaging purposes, as long as the rate of its production via AChE hydrolysis remained rate-limiting. As these esters are substrates for an enzyme, it will also be of considerable interest to determine if the apparent in vivo rate of hydrolysis is dependent on endogenous substrate levels; in this regard, we have done experiments showing that the in vivo hydrolysis of [^{11}C]PMP, as measured via regional brain distributions at 10 min, is unaffected ($P > 0.5$) by the specific activity of the injected radiotracer (100- and 1,000-fold dilutions of specific activity; data not shown). This is consistent with the very high catalytic rate for AChE, which has been described as nearing the limits of the rate of diffusion of molecules through the medium; with such a catalytic rate (estimated at 25,000 molecules/s for acetylcholine; Hucho et al., 1991), the residence time of substrates at the active site is so short (40 μs) that competition of endogenous ACh or added substrate for a radiotracer (such as [^{11}C]PMP) should be unlikely. Such a high rate of enzyme hydrolysis, however, presents new challenges to pharmacokinetic modeling, as this rate becomes the k_3 term in a conventional three-compartmental model; delivery dependency of a tracer is highly dependent on the ratio of k_3 to k_2 (k_2 = rate of egress from the tissue) (Koeppe et al., 1994). We feel [^{11}C]AMP is an example of a tracer suffering from this delivery limitation due to a very high k_3, but that [^{11}C]PMP with a lower rate of hydrolysis may not be delivery limited in any brain region; further studies will be needed to verify these conclusions.

The use of these piperidyl esters in vivo represents a new approach to measuring regional brain AChE activity, but the concept is quite similar to the colorimetric (Johnson and Russell, 1975) and radiometric (Thomsen et al., 1989) methods for in vitro measurements of AChE enzymatic activity. In all of these methods, the rate of

hydrolysis of acetylcholine or an acetylcholine derivative is determined using methods to detect one of the hydrolysis products. Both in vivo and in vitro methods for measuring AChE activity are complementary to the in vitro immunohistochemical methods for AChE (Mesulam et al., 1984; Hammond and Brimijoin, 1988) or in situ hybridization studies of AChE mRNA (Landwehrmeyer et al., 1993; Hammond et al., 1994). In general, it has been assumed that measures of AChE protein and measures of AChE enzymatic activity are highly correlated, and that has been found to be true using in vitro assays of the two different measures in normal and diseased human brain (Hammond and Brimijoin, 1988).

These carbon-11 labeled *N*-methylpiperidyl esters should form a valuable new approach to the study of the cholinergic system, providing estimates of AChE activity which will be complementary to existing methods for in vivo imaging and quantification of the binding of radioligands to muscarinic and nicotinic acetylcholine receptors, vesicular acetylcholine transporters, and the AChE active site. It will now be of considerable interest to study the possible parallel or differential changes of these markers in animal models of neuronal degeneration, and in human Alzheimer's disease brains.

ACKNOWLEDGMENTS

This work was supported by National Institutes of Health grants NS24896, NS15655 and T-32-CA09015 (to S.E.S.), and Department of Energy grant DOE-DE-FG021-87ER60561. The authors thank Drs. Robert A. Koeppe, Guy Bormans, and Kirk A. Frey for helpful discussions.

REFERENCES

Arnett, C.D., Fowler, J.S., MacGregor, R.R., Schlyer, D.J., Wolf, A.P., Langstrom, B., and Halldin C. (1987) Turnover of brain monoamine oxidase measured in vivo by positron emission tomography using L-[^{11}C]deprenyl. J. Neurochem., 49:522–527.

Bierer, L.M., Haroutunian, V., Gabriel, S., Knott, P.J., Carlin, L.S., Purohit, D.P., Perl, D.P., Schmeidler, J., Kanof, P., and Davis, K.L. (1995) Neurochemical correlates of dementia severity in Alzheimer's disease: Relative importance of the cholinergic defecits. J. Neurochem., 64:740–760.

Chen, Y.L., Nielsen, J., Hedberg, K., Dunaiskis, A., Jones, S., Russo, L., Johnson, J., Ives, J., and Liston, D. (1992) Syntheses, resolution and structure-activity relationships of potent acetylcholinesterase inhibitors: 8-carbaphysostigmine analogues. J. Med. Chem., 35: 1429–1434.

Dewey, S.L., MacGregor, R.R., Brodie, J.D., Bendreim, B., King, P.T., Volkow, N.D., Schlyer, D.J., Fowler, J.S., Wolf, A.P., Gatley, S.J., and Hitzemann, R. (1990) Mapping muscarinic receptors in human and baboon brain using [*N*-^{11}C-methyl]-benztropine. Synapse, 5:213–223.

Durkin, T., Ayad, G., Ebel, A., and Mandel, P. (1977) Regional acetylcholine turnover rates in the brains of three inbred strains of mice: Correlations with some inter-strain behavioural differences. Brain Res., 136:475–486.

Eckelman, W.C., Reba, R.C., Rzeszotarski, W.J., Gibson, R.E., Hill, T., Holman, B.L., Budinger, T.F., Conklin, J.J., Eng, R., and Grissom, M.P. (1984) External imaging of cerebral muscarinic acetylcholine receptors. Science, 223:291–293.

Frey, K.A., Ciliax, B., and Agranoff, B.W. (1991) Quantitative in vivo receptor binding IV. Detection of muscarinic receptor down-regulation by equilibrium and by tracer kinetic methods. Neurochem. Res., 16:1017–1023.

Frey, K.A., Koeppe, R.A., Mulholland, G.K., Jewett, D.M., Hichwa, R.E., Ehrenkaufer, R.L.E., Carey, J.E., Wieland, D.M., Kuhl, D.E. and Agranoff, B.W. (1992) In vivo muscarinic cholinergic receptor imaging in human brain with [^{11}C]scopolamine and positron emission tomography. J. Cereb. Blood Flow Metab., 12:147–154.

Glowinski, J., and Iversen, L.L. (1966) Regional studies of cetecholamines in the rat brain-1. J. Neurochem., 13:655–676.

Gordon, M.N., and Finch, C.E. (1984) Topochemical localization of choline acetyltransferase and acetylcholinesterase in mouse brain. Brain Res., 308:364–368.

Hammond, P., and Brimijoin, S. (1988) Acetylcholinesterase in Huntington's and Alzheimer's disease: Simultaneous enzyme assay and immunoassay of multiple brain regions. J. Neurochem., 50: 1111–1116.

Hammond, P., Rao, R., Koenigsberger, C., and Brimijoin, S. (1994) Regional variation in expression of acetylcholinesterase mRNA in adult rat brain analyzed by in situ hybridization. Proc. Natl. Acad. Sci. USA, 91:10933–10937.

Hucho, F., Jarv, J., and Wiese, C. (1991) Substrate-binding sites in acetylcholinesterase. Trends Pharmacol. Sci., 12:422–426.

Irie, T., Fukushi, K., Akimoto, Y., Tamagami, H., and Nozaki, T. (1994) Design and evaluation of radioactive acetylcholine analogs for mapping brain acetylcholinesterase (AChE) in vivo. Nucl. Med. Biol., 21:801–808.

Johnson, C.D., and Russell, R.L. (1975) A rapid, simple radiometric assay for cholinesterase, suitable for multiple determinations. Anal. Biochem., 64:229–238.

Jung, Y.-W., Van Dort, M.E., Gildersleeve, D.L., and Wieland, D.M. (1990) A radiotracer for mapping cholinergic neurons of the brain. J. Med. Chem., 33:2065–2068.

Kilbourn, M.R., Jung, Y.-W., Haka, M.S., Gildersleeve, D.L., Kuhl, D.E., and Wieland, D.M. (1990) Mouse brain distribution of a carbon-11 labeled vesamicol derivative: Presynaptic marker of cholinergic neurons. Life. Sci., 47:1955–1963.

Koeppe, R.A., Frey, K.A., Mulholland, G.K., Kilbourn, M.R., Buck, A., Lee, K.S., and Kuhl, D.E. (1994) [^{11}C]Tropanyl benzilate-binding to muscarinic cholinergic receptors: Methodology and kinetic modeling alternatives. J. Cereb. Blood Flow Metab., 14:85–99.

Kuhl, D.E., Koeppe, R.A., Fessler, J.A., Minoshima, S., Ackermann, R.J., Carey, J.E., Gildersleeve, D.L., Frey, K.A., and Wieland, D.M. (1994) In vivo mapping of cholinergic neurons in the human brain using SPECT and IBVM. J. Nucl. Med., 35:405–410.

Landwehrmeyer, B., Probst, A., Palacios, J.M., and Mengod, G. (1993) Expression of acetylcholinesterase messenger RNA in human brain: An in situ hybridization study. Neuroscience, 57:615–634.

Mesulam, M.-M., Mufson, E.J., Levey, A.I., and Wainer, B.H. (1984) Atlas of cholinergic neurons in the forebrain and upper brainstem of the macaque based on monoclonal choline acetyltransferase immunohistochemistry and acetylcholinesterase histochemistry. Neuroscience, 12:669–686.

Mueller-Gartner, H.W., Wilson, A.A., Dannals, R.F., Wagner, H.N., and Frost, J.J. (1992) Imaging muscarinic cholinergic receptors in human brain in vivo with SPECT, [^{123}I]-4-iododexetimide and [^{123}I]-4-iodolevetimide. J. Cereb. Blood Flow Metab., 12:562–570.

Mueller-Gartner, H.W., Mayberg, M.S., Fisher, R.S., Lesser, R.P., Wilson, A.A., Ravert, H.T., Dannals, R.F., Wagner, H.N. Jr., Uematsu, S. and Frost, J.J. (1993) Decreased hippocampal muscarinic cholinergic receptor binding measured by ^{123}I-iododexetimide and single-photon emission computed tomography in epilepsy. Ann. Neurol., 34:235–238.

Mulholland, G.K., Otto, C.A., Jewett, D.M., Kilbourn, M.R., Koeppe, R.A., Sherman, P.S., Petry, N.A., Carey, J.E., Atkinson, E.R., Archer, S., Frey, K.A., and Kuhl, D.E. (1992) Synthesis, rodent biodistribution, dosimetry, metabolism and monkey images of carbon-11-labeled (+)-2α-tropanyl benzilate: A central muscarinic receptor imaging agent. J. Nucl. Med., 33:423–430.

Namba, H., Irie, T., Fukushi, K., and Iyo, M. (1994) In vivo measurement of acetylcholinesterase activity in the brain with a radioactive acetylcholine analog. Brain Res., 667:278–282.

Rogers, G.A., Stone-Elander, S., Ingvar, M., Eriksson, L., Parson, S.M., and Widen, L. (1994) ^{18}F-Labeled vesamicol derivatives: Syntheses and preliminary in vivo small animal positron emission tomography evaluation. Nucl. Med. Biol., 21:219–230.

Smolen, A., Smolen, T.N., Wehner, J.M., and Collins, A.C. (1985) Genetically determined differences in acute responses to diisopropylfluorophosphate. Pharmacol. Biochem. Behav., 22:623–630.

Smolen, A., Smolen, T.N., Han, P.C., and Collins, A.C. (1987) Sex differences in the recovery of brain acetylcholinesterase activity following a single exposure to DFP. Pharmacol. Biochem. Behav., 26:813–820.

Suhara, T., Inoue, O., Kobayashi, K., Suzuki, K., and Tateno, Y. (1993) Age-related changes in human muscarinic acetylcholine receptors

measured by positron emission tomography. Neurosci. Lett., 149:225–228.

Tavitian, B., Pappata, S., Planas, A.M., Jobert, A., Bonnot-Lours, S., Crouzel, C., and DiGiamberardino, L. (1993) In vivo visualization of acetylcholinesterase with positron emission tomography. NeuroReport, 4:535–538.

Thomsen, T., Kewitz, H., and Pleul, O. (1989) A suitable method to monitor inhibition of cholinesterase activities in tissues as induced by reversible enzyme inhibitors. Enzyme, 42:219–224.

Varastet, M., Brouillet, E., Prenant, C., Crouzel, C., Stulzaft, O., Bottlaender, M., Cayla, J., Maziere, B., and Maziere, M. (1992) In vivo visualization of central muscarinic receptors using [^{11}C]quiniclidinyl benzilate and positron emission tomography in baboons. Eur. J. Pharmacol., 213:275–284.

Virgili, M., Contestabile, A., and Barnabei, O. (1991) Postnatal maturation of cholinergic markers in forebrain region of C57BL/6 mice. Dev. Brain Res., 63:281–285.

Widen, L., Eriksson, L., Ingvar, M., Parsons, S.M., Rogers, G.A., and Stone-Elander, S. (1993) PET studies of central cholinergic nerve terminals in animals and man. J. Cereb. Blood Flow Metab., 13:S300.

Wilson, A.A., Scheffel, U.A., Dannals, R.F., Stathis, M., Ravert, H.T., and Wagner, H.N. (1991) In vivo biodistribution of two [^{18}F]-labeled muscarinic cholinergic receptor ligands: 2-[^{18}F]- and 4-[^{18}F]-fluorodexetimide. Life Sci., 48:1385–1394.

Wyper, D.J., Brown, D., Patterson, J., Owens, J., Hunter, R., Teasdale, E., and McColluch, J. (1993) Defecits in iodine-labelled 3-quiniclidinyl benzilate binding in relation to cerebral blood flow in patients with Alzheimer's disease. Eur. J. Nucl. Med., 20:379–386.

Yoshida, T., Ichiya, Y., Kuwabara, Y., Sasaki, M., Fukumura, T., Ichimya, A., Takita, M., and Masuda, K. (1995) The semiquantiative cerebral cholinergic receptor measurement of patients with Alzheimer's disease and dementia of Alzheimer's type using C-11-NMPB. J. Nucl. Med., 3:238P.

Zubieta, J.K., Frey, K.A., Koeppe, R.A., Kilbourn, M.R., Mulholland, G.K., Foster, N.L., and Kuhl, D.E. (1994) Muscarinic receptor binding in aging and Alzheimer's disease determined with [C-11] *N*-methyl-4-piperidyl benzilate and PET. J. Nucl. Med., 35:20P.